Background

Poly(ADP-ribose) polymerase-1 (Parp-1) is a nuclear protein that catalyzes the transfer of ADP-ribose units to various nuclear proteins as a post-translational modification [1]. Poly (ADP-ribose) is a highly negatively charged molecule and poly (ADP-ribosylation) of chromatin-bound proteins including histone may change the interaction of the modified proteins with DNA or other proteins. A 'histone shuttle model' proposed by Althaus et al. can explain the dynamic changes of chromatin structure through histone replacement induced by Parp-1 activation [2]. Accumulating evidence suggests that under *Parp-1* deficiency, transcriptional regulation, cell differentiation, and tumorigenesis are substantially affected. For example, Parp-1 is involved in the regulation of *Reg3* gene [3] as a transcription factor. As a co-activator, Parp-1 plays a role in the regulation of ligand-induced transactivation of ecdysone receptor [4], and in the transcriptional control of the target genes by AP-2 [5], and by MYB [6]. As a co-repressor, Parp-1 regulates the expression of RXR-regulated genes [7] and also plays an auto-regulatory role in the transcription of the *Parp-1* gene itself [8]. Parp-1 also modulates the activity of the transcription factor NF-κB and consequently, the expression of NF-κB-dependent genes, including *inducible nitric oxide synthetase* (*iNOS*) [9]. The expression of nearly 1% of the genes, including those involved in cell cycle control and DNA replication was affected in exon 2 disrupted *Parp-1*$^{-/-}$ mouse embryonic fibroblasts (EF cells) [10]. *Parp*-deficient *Drosophila* showed attenuation of gene expression located in puff loci and also lost puff formation, suggesting a role for Parp in the induction of genes located at specific chromosomal loci [11].

Recent studies further suggest that Parp-1 is involved in the regulation of dynamic changes of gene expression induced by specific stimuli. Parp-1 is associated with transcriptionally repressed chromatin domains, which do not overlap with the regions where histone H1 is located [12]. NAD-dependent alteration of chromatin structure through Parp-1 auto-modification was demonstrated to lead to activation of estrogen induced estrogen receptor dependent transcription [12]. In addition, the PARP inhibitor, 3-aminobenzamide induced hypermethylation of the *Htf9* gene, suggesting the presence of a negative correlation between poly(ADP-ribosylation) and DNA methylation [13]. In spite of the above evidence, how Parp-1 is involved in the epigenetic regulation and functions in the maintenance of basal gene expression profiles of cells are not well understood.

We previously reported induction of the trophoblast lineage in exon 1 disrupted *Parp-1*$^{-/-}$ ES cells during teratocarcinoma-like tumor formation [14], as well as *in vitro* culture [15]. Simultaneous induction of several trophoblast marker genes, including *placental lactogen I* and *II*, *proliferin* and *Tpbp* (*4311*) in *Parp-1*$^{-/-}$ ES cells took place without any stimulus during trophoblast induction [15]. We therefore considered that ES cells as well as tissues in live mice might be good material in which to study the effects of *Parp-1* deficiency on a basal level of gene expression, namely epigenetic regulation, at the genome-wide level. In this study, global gene expression profiles were studied in exon 1 disrupted *Parp-1*$^{-/-}$ ES cells as well as in the livers of mice.

Results and discussion

Gene expression profile in Parp-1$^{-/-}$ *ES cells*

A comparison of the basal gene expression profiles in *Parp-1*$^{-/-}$ *ES cells* to their wild-type (*Parp-1*$^{+/+}$) counterparts, is presented in Fig. 1A–C and Table 1. We found the expression of (950/9,907) genes, namely 9.6%, was different by at least 2-fold between *Parp-1*$^{-/-}$ and *Parp-1*$^{+/+}$ ES cells ($p < 0.05$) (Fig. 1B and Table 1). Notably, a larger fraction of the genes, 6.3% (626/9,907) was down-regulated, whereas only 3.3% (324/9,907) of the genes were up-regulated (see Table 1).

We also made the heatmaps using the gene lists containing the 928 genes that showed a difference at $p < 0.01$ in ES cells (Fig. 2A). Although we used independently isolated *Parp-1*$^{-/-}$ ES cell clones, a clear common alteration in the gene expression profile was observed (see Fig. 2A, and Tables 2 and 3).

We further selected the genes that showed relatively high expression levels (the "Flag value" in GeneSpring ver. 6.1 of the genes should be either "Present" (high level of expression) or "Marginal" (moderate level of expression) in all six replicates of the genotype within the 928 genes that showed a difference at $p < 0.01$, see Table 1). Among the 86 genes that this analysis identified, there were 62 genes, obviously including the Parp-1 (Adprt1) gene itself, that were down-regulated and 24 genes up-regulated, as listed in Tables 2 and 3. Reduced expression of Igfbp3 (insulin-like growth factor binding protein 3) and Galnt1 (polypeptide GalNAc transferase-T1) in Parp-1-/- ES cells was further confirmed by Northern blot analysis (Fig. 3A). These down- and up-regulated genes in Parp-1-/- ES cells are involved in a variety of cellular processes, including transcription, metabolism, signaling, immune response, cell structure, and other cellular processes (Fig. 3B, and Tables 2 and 3).

Gene expression profile of the livers and EF cells

In the livers, 3.3% (411/12,353) of genes showed a significant difference in expression level ($p < 0.05$) between the *Parp-1* genotypes. In the livers of *Parp-1*$^{-/-}$ mice, 2.0% (253/12,353) of the genes were down-regulated and 1.3% (158/12,353) of the genes were up-regulated ($p < 0.05$).

Table 1: Differential expression of genes between *Parp-1*$^{+/+}$ and *Parp-1*$^{-/-}$ ES cells, livers, and EFs

	No. of genes				
		Parp-1$^{-/-}$ <*Parp-1*$^{+/+}$		*Parp-1*$^{-/-}$ > *Parp-1*$^{+/+}$	
p-value cut off[a]	Total	Total	2-fold or greater	Total	2-fold or greater
ES cells[c]					
Total[b]	9,907	5,464	1,283	4,349	1,406
$p < 0.05$[b]	2,273	1,609	626	664	324
$p < 0.01$[b]	928	684	259	244	120
Livers[d]					
Total[b]	12,353	7,138	1,184	4,860	1,038
$p < 0.05$[b]	1,616	1,190	253	426	158
$p < 0.01$[b]	641	515	100	126	43
EFs[e]					
Total	12,359	5,042	707	7,317	501
$p < 0.05$	996	390	216	606	205

[a] Analyzed by One-Way ANOVA (non-parametric test known as Wilcoxon-Mann-Whitney test)
[b] These genes were presented in Fig. 1 (A)-(F).
[c] *Parp-1*$^{+/+}$ ES cell clone, J1, and *Parp-1*$^{-/-}$ ES cell clones, 210-58 and 226-47, were used.
[d] Two mice were used for each genotype.
[e] Three EFs obtained from three embryos were analyzed as triplicate experiments.

Similar to *Parp-1*$^{-/-}$ ES cells, a higher percentage of the genes, 62% (253/411), were down-regulated and the remaining 38% were up-regulated (Fig. 1D–F, and Table 1). The expression of representative marker genes of the liver, including *albumin* (*Alb1*) and *phosphoenolpyruvate carboxykinase* (*Pepck*) was similarly high in both *Parp-1* genotypes.

The heatmaps were constructed using the gene lists containing the 641 genes that showed a difference at $p < 0.01$ in livers (Fig. 2B). *Parp-1* deficiency commonly altered gene expression profiles in the livers of two mice analyzed (Fig. 2B, Table 4). Among 641 genes, we identified 26 genes that showed a relatively high level of expression (genes with "Flag values" of either "Marginal" or "Present" in each genotype) and were altered 2-fold or greater between the *Parp-1*$^{-/-}$ and *Parp-1*$^{+/+}$ livers ($p < 0.01$) (Table 4). Among them, 15 genes were down-regulated and 11 genes were up-regulated.

In the case of the EF cells, the results obtained from these 3 replicates are shown in Table 1. In *Parp-1*$^{-/-}$ EF cells, 1.7% (216/12,359) and 1.7% (205/12,359) genes were down- and up-regulated, respectively ($p < 0.05$). We were not able to construct gene lists with a p value less than $p < 0.02$.

Comparison of the profiles among different cell types

We compared gene expression profiles between *Parp-1*$^{-/-}$ ES cells and the livers. There were no commonly up- or down-regulated genes in Tables 2, 3, 4, namely in the genes showing relatively high expression levels selected by Flag values, although we observed that 20 genes including *Eif2s2* (*eukaryotic translation initiation factor 2 subunit 2 beta*), *Parp-1*, and 6 genes were commonly down- and up-regulated in the ES cells and livers ($p < 0.05$), respectively (Fig. 2C–F). There was no gene commonly altered in ES cells, livers, and EFs. Comparison of the affected genes in the ES cells, livers, and EF cells thus revealed that *Parp-1*-deficiency mostly altered the expression level of different sets of genes depending on the cell types.

Up-regulation of the differentiation pathway to extraembryonic tissues in Parp-1$^{-/-}$ *ES cells*

Among the genes, we found up-regulation of *H19, Sparc, Sox17, and Gata6* in *Parp-1*$^{-/-}$ ES cells (Table 3). The *H19* gene has been suggested to regulate differentiation into extraembryonic tissues including trophoblast lineage and extraembryonic endoderms [16-18]. *Sparc, Sox17,* and *Gata6* are known as marker genes of extraembryonic endoderms [19-21]. Because we previously reported induction of trophoblast lineage in untreated *Parp-1*$^{-/-}$ ES cells during *in vitro* culture, we speculated that a higher level of *H19* expression in *Parp-1*$^{-/-}$ ES cells may be involved in induction of extraembryonic tissues including trophoblast lineage. The mouse *H19* gene is located on the distal region of chromosome 7 and encodes the 2.3 kb untranslated transcript, which is maternally expressed, and the *H19* gene and the *insulin-like growth factor 2* (*Igf2*) gene are reciprocally imprinted [22].

We analyzed expression of *H19* and *Igf2* genes in untreated *Parp-1*$^{-/-}$ and *Parp-1*$^{+/+}$ ES cell lines by semi-quantitative RT-PCR (Fig. 4A). We confirmed that the *H19*

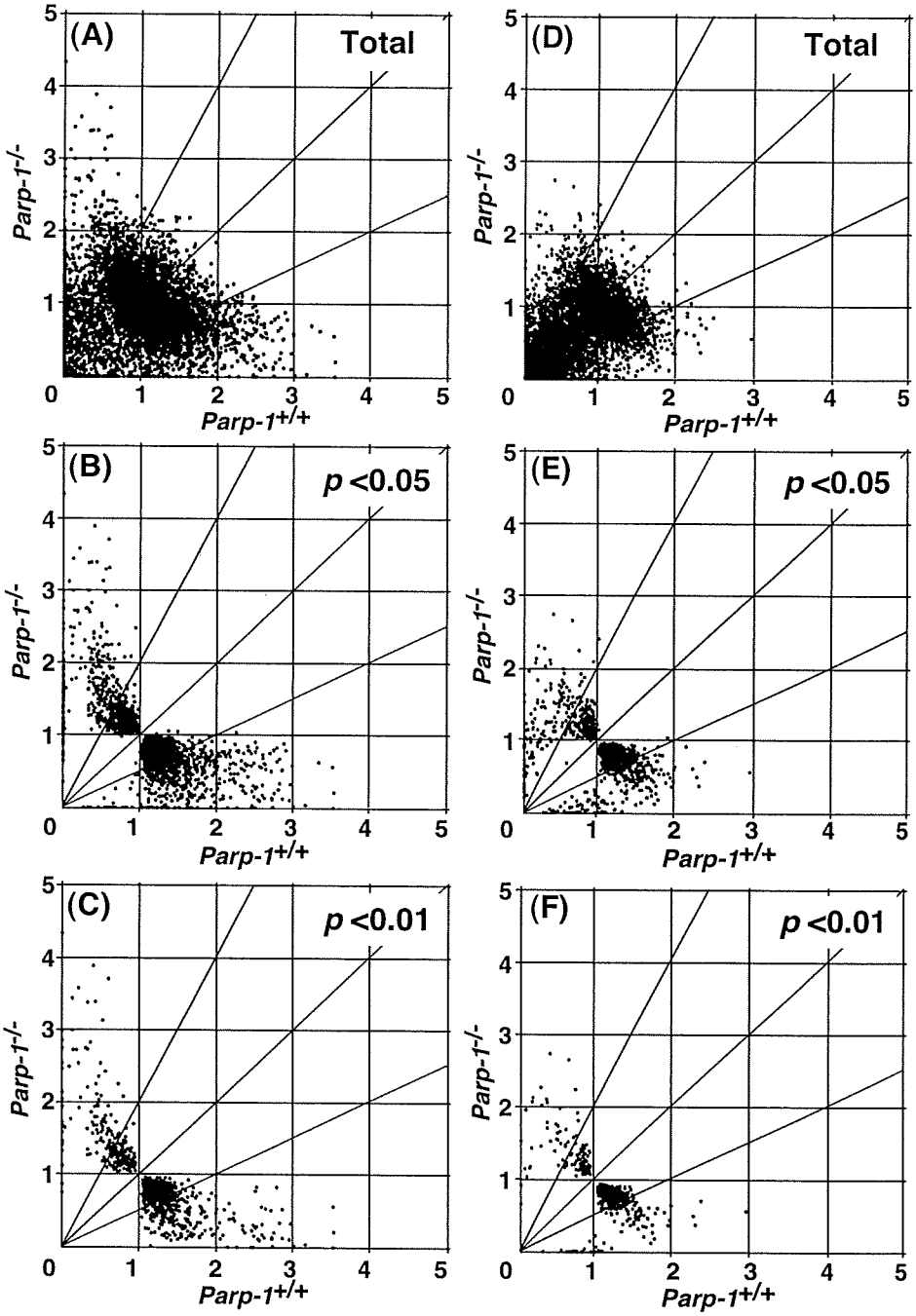

Figure 1

Effect of *Parp-1* deficiency on gene expression. Gene expression data from microarray analyses are plotted for *Parp-1*$^{-/-}$ versus wild-type (*Parp-1*$^{+/+}$) ES cell lines (A-C) or the livers (D-F). Horizontal and vertical axes represent expression levels normalized for an individual gene. Each point represents normalized expression data for an individual gene. The genes that showed standard deviations greater than 2.0 in the normalized data of both genotypes (A and D) were excluded and gene lists were constructed with $p < 0.05$ (B and E), or $p < 0.01$ (C and F).

Table 2: Genes down-regulated in *Parp-1*$^{-/-}$ ES cells

Accession No.	Fold change[a]			Symbol	Chromosome	Gene description
	W vs H	J1 vs 210-58	J1 vs 226-47			
Cell cycle/cell proliferation/cell death						
AW122355	3.2	5.2	2.3	*Prkcbp1*	2	Protein kinase C binding protein 1
AF067395	2.9	2.9	2.9	*Bnip3l*	14	BCL2/adenovirus E1B 19 kDa-interacting protein
AI842277	2.7	2.3	3.2	*Igfbp3*	11	Insulin-like growth factor binding protein 3
U95826	2.2	2.5	1.9	*Ccng2*	5	Cyclin G2
Cell structure/cell adhesion						
U16741	4.1	6.3	3.1	*Capza2*	6	Capping protein (actin filament) muscle Z-line, alpha 2
AI132380	3.6	3.1	4.3	*Fndc3a*	14	Fibronectin type III domain containing 3a
AI505453	2.9	2.5	3.4	*Myh9*	15	Myosin, heavy polypeptide 9, non-muscle
AW208938	2.4	3.2	2.0	*Pkp2*	16	Plakophilin 2
M76124	2.4	2.2	2.6	*Tacstd1*	17	Tumor-associated calcium signal transducer 1
Metabolism						
U73820	5.5	5.2	5.8	*Galnt1*	18	Polypeptide GalNAc transferase-T1 (ppGaNTase-T1)
AI841270	3.4	2.4	6.4	*Gstm1*	3	Glutathione S-transferase, mu1
AV308550	2.6	4.1	1.9	*Piga*	x	Phosphatidylinostitol glycan, class A
AI851912	2.3	2.2	2.5	*Rps27*	3	Ribosomal protein S27
AI852144	2.1	2.9	1.7	*Pbef-pending*	12	Pre-B-cell colony-enhancing factor
U65986	2.1	1.9	2.5	*Anxa11*	14	Annexin A11
D50264	2.1	1.4	4.1	*Pigf*	17	Phosphatidylinositol glycan, class F
AF031486	2.0	2.0	2.0	*Sms*	x	Spermidine synthase
AI845882	2.0	2.5	1.7	*Acyp1*	12	Acylphosphatase1, erythrocyte (common) type
Protein biosynthesis/degradation						
AI852581	3.0	3.0	3.1	*Ide*	19	Insulin degradating enzyme
AI414051	3.0	1.8	9.1	*Usp24*	4	Ubiquitin specific protease 24
AW121012	2.9	2.8	2.8	*Rnf19*	15	Ring finger protein 19
X92665	2.9	2.5	3.4	*Ube2e1*	14	Ubiquitin-conjugating enzyme UbcM3
AW048882	2.2	2.8	1.8	*Iars*	13	Isoleucine-tRNA synthetase
AA867340	2.2	1.9	2.6	*Psme4*	11	Proteasome (prosome, macropain) activator subunit
AB024427	2.2	2.3	2.1	*Rnf11*	4	Ring finger protein 11
Signaling						
AI846023	4.6	2.8	13.1	*Arl7*	1	ADP-ribosylation factor-like 7
AA260005	2.8	2.7	2.8	*Pawr*	10	PPKC, apoptosis, WT1, regulator
AI317205	2.6	2.4	2.7	*Map3k1*	13	Mitogen activated protein kinase kinase kinase 1
AF035644	2.3	2.0	2.7	*Ptp4a2*	4	Protein tyrosine phosphatase 4a2
M21019	2.3	1.9	2.9	*Rras*	7	Harvey rat sarcoma oncogene, subgroup R
AI194248	2.2	2.5	1.9	*Csnk2a1*	2	Casein kinase II, alpha 1 polypeptide
AI854006	2.0	2.0	2.1	*Set*	2	SET translocation
D83921	2.0	1.9	2.1	*Ebaf*	1	Endometrial bleeding associated factor
Transcription/replication						
X14206	9.9	8.4	12.0	*Adprt1*	1	Poly(ADP-ribose) polymerase 1
M99167	3.0	6.2	2.0	*Hnrpa1*	15	Heterogeneous nuclear ribonucleoprotein A1

Table 2: Genes down-regulated in *Parp-1*$^{-/-}$ ES cells *(Continued)*

AW107922	2.8	3.7	2.2	*Sox11*	12	SRY box-containing gene 11
AI849135	2.5	2.5	2.5	*Foxo3a*	10	Forkhead box 03a
Y07836	2.5	2.3	2.8	*Bhlhb2*	6	Basic-helix-loop-helix domain containing, class B2
X74760	2.5	2.3	2.7	*Notch3*	17	Notch gene homolog 3, (Drosophila)
AI447783	2.1	2.4	1.9	*Helb*	10	Helicase(DNA) B
X94694	2.1	2.7	1.7	*Tcfap2c*	2	Transcription factor AP-2, gamma
AF077861	2.1	2.2	2.1	*Id2*	12	Inhibitor of DNA binding 2
AI605405	2.0	1.9	2.2	*Phf13*	4	PHD finger protein 13
D78382	2.0	1.7	2.6	*Tob1*	11	Transducer of ErbB2.1
Transport						
AV356315	4.1	5.5	3.3	*Lman1*	18	Lectin, mannose-binding, 1
AV298789	2.9	2.6	3.2	*Ranbp5*	14	Ran binding protein 5
D88315	2.2	2.2	2.2	*Hiat1*	3	Hippocampus abundant gene transcript 1
Unknown						
AI845617	3.5	3.5	3.4	*2610019A05Rik*	11	Hypothetical protein
AI852287	3.2	3.3	3.2	*Ankrd28*	14	Ankyrin repeat domain 28
AI836771	3.0	2.8	3.3	*2900008M13 Rik*	15	Unknown EST
AA684456	2.9	2.1	4.5	*2310015N07Rik*	7	Hypothetical protein
AI848435	2.8	1.9	4.8	*C78339*	13	Unknown EST
AW123157	2.7	2.5	3.1	*1700051E09Rik*	11	Hypothetical protein
AW124843	2.6	3.1	2.3	*C85108*	4	Unknown EST
AA710439	2.6	2.0	3.6	*6230421P05Rik*	16	Unknown EST
AI853444	2.5	1.8	3.9	*2610042L04Rik*	14	Hypothetical protein
AI853444	2.2	2.1	2.3	*2610042L04Rik*	14	Hypothetical protein
AW121353	2.1	1.6	3.1	*Lrrc8*	2	Luecine rich repeat containing 8
AI037493	2.1	1.5	3.4	*Tbc1d15*	10	TBC1 domain family, member 15
AI461803	2.1	2.2	1.9	*1300006C19Rik*	9	Hypothetical protein
AW049969	2.0	2.0	2.1	*C330005L02Rik*	9	Hypothetical protein
AI847483	2.0	2.0	2.0	*Tmem41b*	7	Transmembrane protein 41B

[a]W, wild-type cells (J1); H, *Parp-1*$^{-/-}$ ES cells (210-58 and 226-47).

Table 3: Genes up-regulated in *Parp-1*$^{-/-}$ ES cells

Accession No.	Fold change[a]			Symbol	Chromosome	Gene description
	H vs W	210-58 vs J1	226-47 vs J1			
Cell cycle/cell proliferation/cell death						
X58196	3.1	3.3	2.9	*H19*	7	H19 non-coding RNA
AI842665	3.0	3.1	2.8	*Tax1bp3*	11	Human T-cell leukemia virus type I binding protein 3
Cell structure/cell adhesion						
X04017	2.3	2.3	2.3	*Sparc*	11	Cysteine-rich glycoprotein SPARC
M26071	2.1	2.5	1.8	*F3*	3	Coagulation factor III
M91236	2.1	2.1	2.1	*Gjb5*	4	Gap junction membrane channel protein beta 5
Immune response						
U13705	2.3	2.1	2.4	*Gpx3*	11	Glutathione peroxidase 3
Metabolism						
AW120625	2.3	1.9	2.7	*Pgd*	4	Phosphogluconate dehydrogenase
M64782	2.2	1.9	2.5	*Folr1*	7	Folate-binding protein 1 (FBP1)
X97755	2.0	2.1	2.0	*Ebp*	x	Phenylalkylamine Ca2+ antagonist (emopamil) binding protein
Protein biosynthesis/degradation						
W71352	3.9	4.2	3.6	*Bag2*	1	Bcl2-associated athanogene 2
AI844175	3.4	3.4	3.4	*Mrps11*	7	Mitochondrial ribosomal protein S11
U16163	2.9	2.9	2.8	*P4ha2*	11	Prolyl 4-hydroxylase alpha(II)-subunit
D00622	2.5	2.0	3.0	*Lrpap1*	5	Low density lipoprotein receptor related protein, associated protein 1
X60676	2.3	2.4	2.2	*Serpinh1*	7	HSP47
AW124432	2.1	1.8	2.5	*Mrpl12*	11	Mitochondrial ribosomal protein L12
AI839392	2.0	2.0	2.1	*Aars*	8	Alanyl-tRNA syntase
Transcription/replication						
D49473	3.4	3.0	3.7	*Sox17*	1	SRY-box containing gene 17
U51335	2.5	2.5	2.6	*Gata6*	18	GATA-binding protein 6
U79962	2.4	2.1	2.6	*Tarbp2*	15	TAR (HIV) RNA binding protein 2
D49473	2.1	1.9	2.3	*Sox17*	1	SRY-box containing gene 17
Transport						
D14077	2.2	2.1	2.2	*Clu*	14	Clusterin
Others						
M34603	2.6	2.3	3.0	*Prg*	10	Proteoglycan core protein
AA793009	2.3	2.0	2.7	*Tex19*	11	Testis expressed gene 19
Unknown						
AI846553	3.2	3.0	3.3	*1110020C13Rik*	15	Hypothetical protein
AI845664	2.1	2.0	2.2	*Grwd*	7	Glutamate-rich WD repeat containing 1

[a] H, *Parp-1*$^{-/-}$ ES cells (210-58 and 226-47); W, wild-type cells (J1).

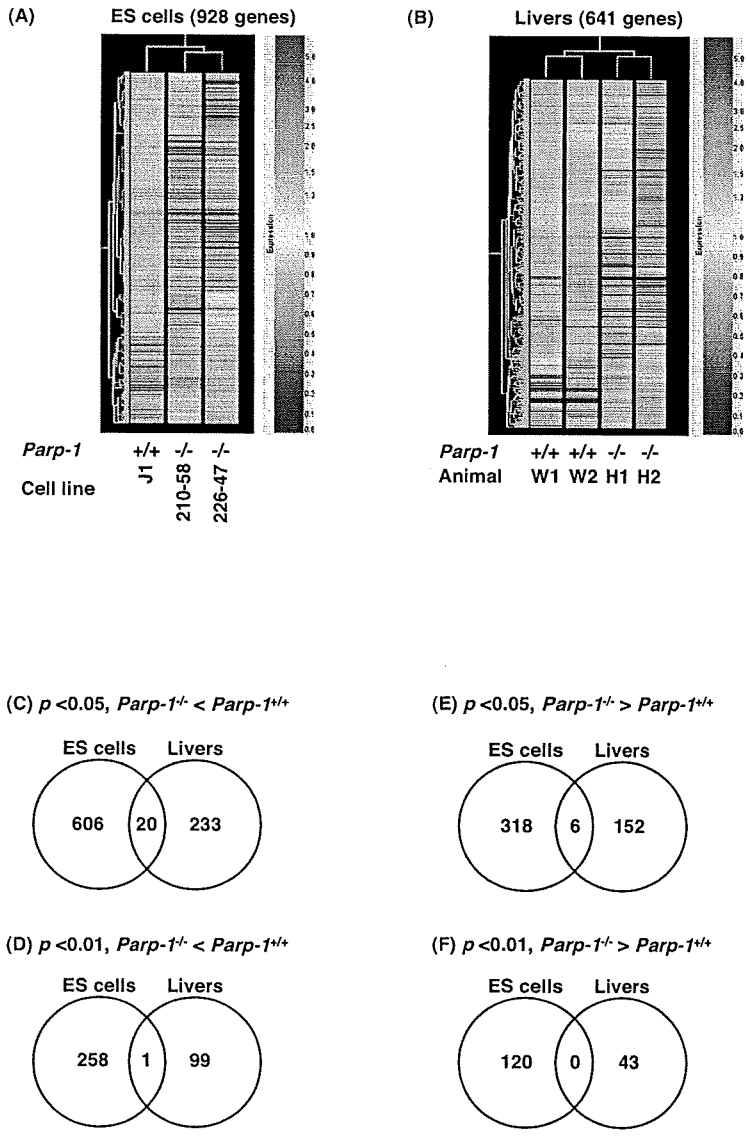

Figure 2

Comparison of gene expression profiles among cell lines, animals, or cell types. Heatmaps of gene expression profiles in ES cells (A) and Livers (B). We constructed the heatmaps using the gene lists containing the genes that showed a difference at $p < 0.01$ in ES cells and livers, respectively. Each heatmap is constructed using GeneSpring GX ver. 7.3.1. Numbers of commonly down- (C & D) or up- (E & F) regulated genes between *Parp-1*$^{-/-}$ ES cells and livers. The numbers of the genes were indicated in Venn diagrams. These genes showed the difference with at least 2-fold between *Parp-1*$^{+/+}$ and *Parp-1*$^{-/-}$ ($p < 0.05$, C & E, or $p < 0.01$, D & F).

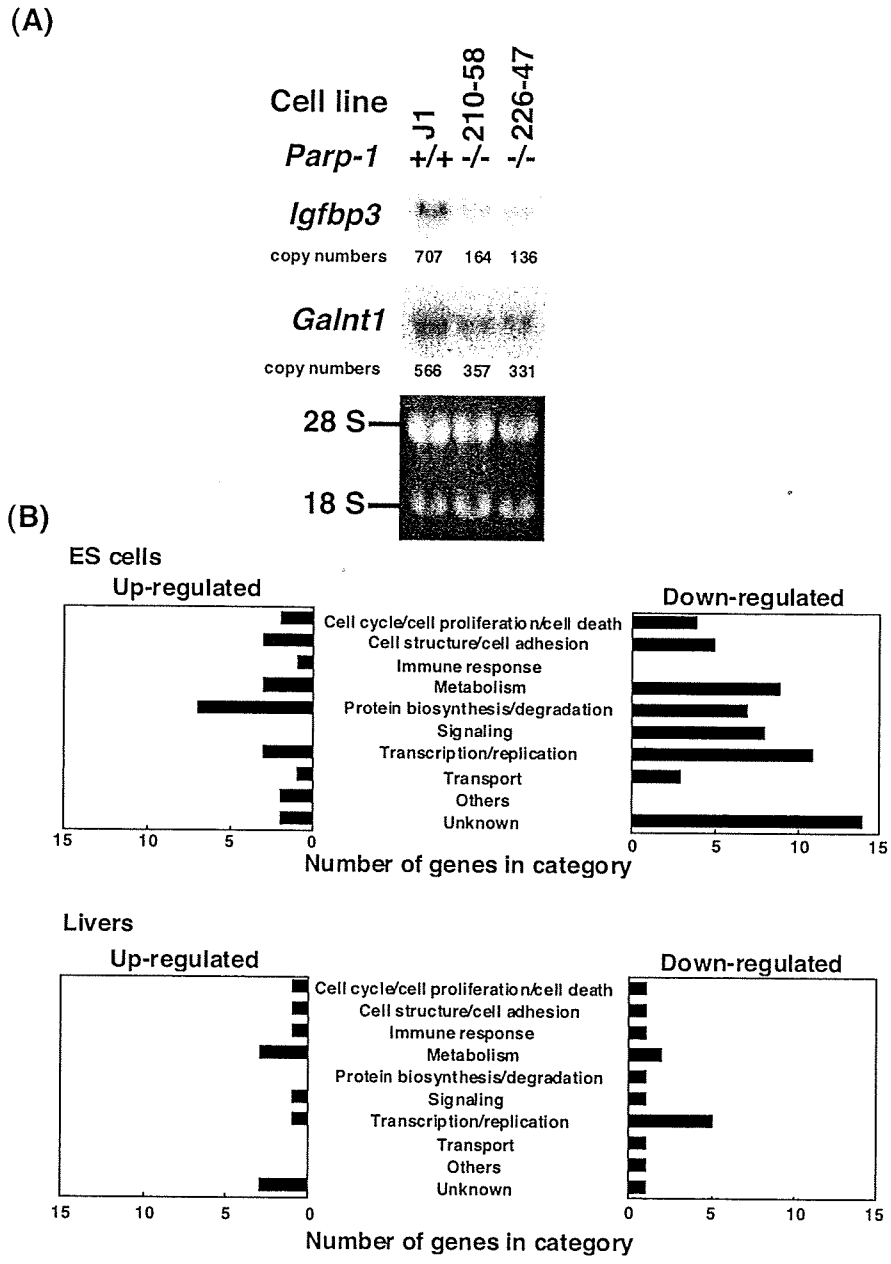

Figure 3
Confirmation of differentially expressed genes in microarray analysis by northern blot analysis (A), and functional categorization of up- and down-regulated genes (B). Ten micrograms of total RNA were used for northern blot analysis in (A). Copy numbers were calculated from the radioactivities of the probe control.

Table 4: Genes down- and up-regulated in *Parp-1*$^{-/-}$ livers

	Accession No.	Fold change[a]					Symbol	Chromosome	Gene description
		W vs H	W1 vs H1	W1 vs H2	W2 vs H1	W2 vs H2			
Down-regulated									
Cell structure/cell adhesion									
	AA867778	2.1	2.4	2.6	1.7	1.8	*Actn1*	12	Actinin, alpha 1
Cell cycle/cell proliferation/cell death									
	AJ223782	2.0	1.8	1.7	2.5	2.3	*Sept7*	9	Septin7 (Cdc10)
Immune response									
	X05475	2.1	2.5	1.8	2.6	1.9	*C9*	15	Complement component C9
Metabolism									
	L42996	3.0	1.7	3.7	2.7	5.8	*Dbt*	3	Nuclear-encoded mitochondrial acyltransferase
	AF026075	2.4	1.8	4.3	1.7	4.0	*Sult3a1*	10	Sulfotransferase-related protein (SULT-X2)
Protein biosynthesis/degradation									
	M27347	3.2	3.4	3.2	3.1	3.0	*Ela1*	15	P6-5 gene, 3' end (elastase 1)
Signaling									
	AI563623	2.3	2.9	1.9	2.9	1.8	*Pkn2*	3	Protein kinase N2
Transcription/replication									
	AF010405	4.9	6.8	3.2	8.5	4.1	*Hfh-1L*	13	HNF-3/forkhead homolog 1 like
	L20450	3.7	3.1	2.7	5.0	4.3	*Zfp97*	17	Zinc finger protein 97
	AW048355	2.1	1.6	1.9	2.3	2.8	*Phf17*	3	PHD finger protein 17
	AI848996	2.1	2.2	2.3	2.0	2.1	*Dhx40*	11	DEAH box polypeptide 40
	AW123909	2.1	1.5	1.9	2.2	2.9	*Rbpms*	8	RNA binding protein gene with multiple splicing
Transport									
	D86066	3.2	2.3	4.4	2.6	4.8	*Rab5ep - pending*	11	Rabaptin-5
Others									
	AI835016	2.4	2.1	2.3	2.5	2.7	*Hps4*	5	Light ear protein (1e)
Unknown									
	AI848841	2.1	2.2	1.6	2.7	2.0	*A23010 6A15Rik*	13	Unknown

Table 4: Genes down- and up-regulated in *Parp-1*$^{-/-}$ livers *(Continued)*

		H vs W	H1 vs W1	H1 vs W2	H2 vs W1	H2 vs W2			
Up-regulated									
Cell cycle/cell proliferation/cell death									
	X95280	3.0	2.8	2.7	3.4	3.2	*G0s2*	1	GOS2-like protein
Cell structure/cell adhesion									
	AI132491	2.1	1.9	2.6	1.6	2.2	*Bysl*	17	Bystin-like
Immune response									
	J00475	3.1	9.2	2.8	4.2	1.3	*Iga*	12	Germline IgH chain gene, DJC region-segment D-FL16.1
Metabolism									
	M63245	3.2	2.8	4.0	2.6	3.7	*Alas1*	9	Amino levulinate synthase (ALAS-H)
	AW121625	2.5	2.8	2.4	2.6	2.3	*Galnt11*	5	Polypeptide GalNAc transferase 11
	Y15003	2.1	1.8	1.9	2.3	2.5	*St3gal5*	6	Beta-galactoside alpha-2,3-sialyltransferase 5
Signaling									
	L76567	4.1	1.8	2.3	5.5	7.0	*Shp1*	4	Shp gene
Transcription/replication									
	AI553024	2.4	2.4	1.5	3.8	2.4	*Zbtb16*	9	Zinc finger and BTB domain containing 16
Unknown									
	AI042964	7.1	7.1	8.4	5.9	7.1	*061000 5C13Rik*	7	Hypothetical protein
	AI593759	3.7	3.0	4.0	3.4	4.6	*953005 1K01Rik*	7	Hypothetical protein
	AI019679	2.3	10.0	1.4	9.4	1.3	*110000 1G20Rik*	11	Hypothetical protein

[a] W, *Parp-*$^{+/+}$ livers from two animals (W1 & W2): H, *Parp-1*$^{-/-}$ livers from two animals (H1 & H2).

gene is up-regulated, whereas the *Igf2* gene, which is reciprocally imprinted was slightly down-regulated in both the two *Parp-1*$^{-/-}$ES cell lines.

H19 is highly expressed in extraembryonic tissues, including placenta and cells quite similar to the parietal endoderm of extraembryonic lineages, during ES cell differentiation [16]. Because withdrawal of LIF during ES cell culture causes differentiation of ES cells [23,24], we further analyzed expression of the *H19* gene and other trophoblast marker genes for 7 days after withdrawal of LIF by semi-quantitative RT-PCR. We observed earlier and greater up-regulation of the *H19* gene in two *Parp-1*$^{-/-}$ ES cells compared to wild-type cells (Fig. 4B). We also observed a higher level of induction of trophoblast stem cell marker gene *caudal-related homeobox 2* (*Cdx2*) [25]. The induction of trophoblast giant cell marker gene, *proliferin* (*Plf*) [26] was only observed in *Parp-1*$^{-/-}$ ES cell lines (Fig. 4B). In contrast, *POU domain, class 5, transcription factor 1* (*Oct3/4*) gene, which is a marker gene of undifferentiated ES cells [27], was gradually down-regulated in both genotypes during differentiation, although the expression level of *Oct 3/4* gene became slightly lower in *Parp-1*$^{-/-}$ than in *Parp-1*$^{+/+}$ ES cell lines at day 7 after withdrawal of LIF (Fig. 4B).

These results suggest that the potential for differentiation into trophoblasts is increased in ES cells under *Parp-1* deficiency.

Possible roles of Parp-1 in global gene expression profiles

Using genome-wide analysis of gene expression in different cell types, we showed that the expression of a number of genes is affected by the loss of *Parp-1* in both ES cells as well as in the liver. The results suggest that Parp-1 may be involved directly or indirectly in maintenance of their regulation of expression. The genes that showed altered expressions in *Parp-1*$^{-/-}$ ES cells, livers and EF cells are mostly different depending on the cell type, and are not apparently clustered at particular loci on specific chromosomes, and both house-keeping and inducible genes were present in the affected gene lists. Functional categorization of the altered genes in *Parp-1*$^{-/-}$ ES cells and livers showed that these genes are involved in various cellular processes (Fig. 3B). The *Parp-1*$^{-/-}$ and *Parp-1*$^{+/+}$ ES cells, which we used showed no difference in growth rate [28] and cell-cycle distribution [29], and the karyotype is the same ($2n = 40$) [28]. In mice, we did not observe any differences in body weight nor in the histology of the livers between *Parp-1* genotypes. Therefore, the differences in gene expression should not be caused indirectly by differences in growth and cell proliferation but might be intrinsic to the absence of Parp-1 molecules. In the case of the EF cells, about 1% of the analyzed genes showed altered levels of expression. We did not observe any genes overlapping between the report on *Parp-1*$^{-/-}$ EF cells disrupted at exon 2 [10], and our present results with the exon 1 disrupted EFs. This may be possibly due to differences in targeting construct, genetic backgrounds or the heterogeneity of EFs.

Accumulating evidence suggests that Parp-1 regulates gene expression by modulating transcriptional factors, including YY1 [30], Oct-1 [31], NF-κB [32], E47 [33], and TEF-1 [34]. In these cases, Parp-1 stimulates loading of these transcriptional factors to cognate target sequences through protein-protein interaction. However, it is noteworthy that the target genes of these transcription factors did not show altered expression in this study. Parp-1 is also able to act as co-activator for retinoic acid receptor (RAR)-mediated transcription of *Rarβ2* gene [35] and β-catenin/TCF4 complex-dependent transcription [36]. In the case of *RXRα* [7], Parp-1 may act as a co-repressor for ligand-induced gene activation. Again, in this study, the target genes for *Rarβ2* or *RXRα* genes were not deregulated in *Parp-1*$^{-/-}$ ES cells and in the livers. It is thus suggested that loss of Parp-1 may affect the maintenance of basal expression level of a wide variety of the genes in ES cells and the livers through different mechanisms from the regulation involving these transcription factors.

In addition, PARP-1 binds to the scaffold/matrix attachment region (S/MARs) containing partially unwound AT-rich sequences that form local non-B structures [37]. PARP-1 binds to other non-B DNA structures including hairpin, cruciform, and loop, and is catalytically activated [38]. The variations of gene promoter/enhancer structure and Parp-1 binding and recruitment in different cell types may be possibly related to the observed differences in the effect of *Parp-1* deficiency on expression profiles.

Since PARP inhibitors are shown to cause hypermethylation of particular genes [13], loss of Parp-1 may possibly cause local changes in DNA methylation pattern during DNA replication and may further affect histone acetylation or methylation, thereby causing genome wide alteration of gene expression after rounds of cell division. In this context, it is notable that similar to the case of *Parp-1*$^{-/-}$ cells, the majority (71%) of differentially expressed genes (153/17,664 genes) was down-regulated in the cells deficient in *Trrap*, a co-factor of histone acetyltransferase [39].

Parp-1 is able to modify histones and contributes to the opening of condensed highly ordered chromatin structures [40]. Furthermore, Parp-1 is a structural component of the transcriptionally repressed state of chromatin, and transcription is reported to be activated by auto-modification activity in an NAD-dependent manner [12]. Therefore, the roles of Parp-1 as a chromatin-modifying factor

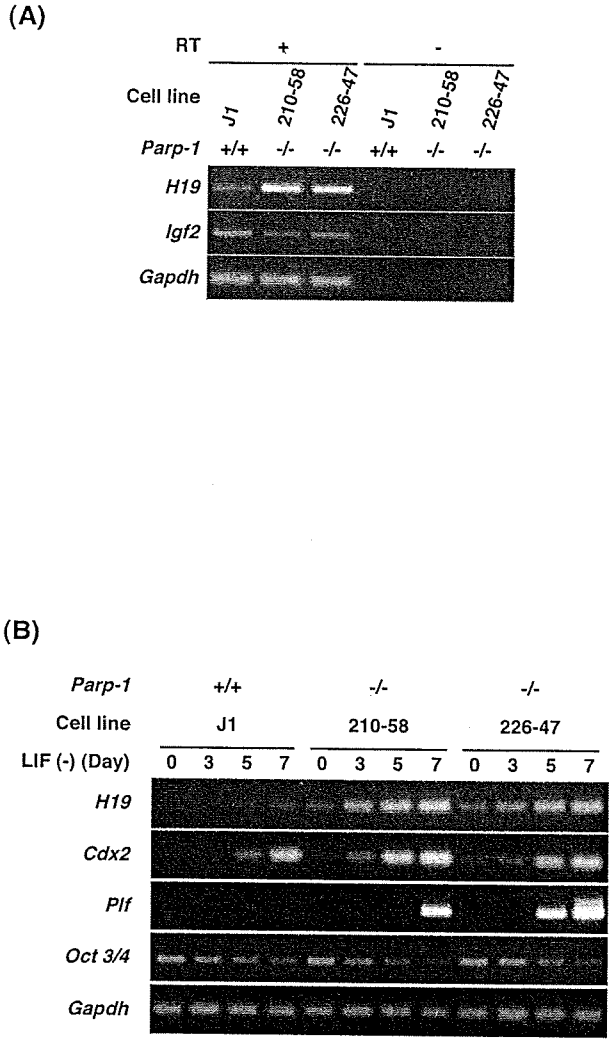

Figure 4

Semi-quantitative RT-PCR analysis of *H19* and other extraembryonic marker gene expression in undifferentiatiated ES cells (A) or during differentiation of ES cells after LIF withdrawal (B). (A) PCR was carried out using cDNA prepared with (+) or without (-) reverse transcriptase (RT) [see Additional file 1 for primers]. (B) Total RNA was prepared using harvested ES cells 3, 5, and 7 days after removal of LIF. RNA samples prepared from untreated ES cells correspond to Day 0. *Gapdh* (*glyceraldehyde-3-phosphate dehydrogenase*) gene was used as an internal control.

may contribute to maintenance of global gene expression during cell proliferation through mechanisms involving polyADP-ribosylation, protein-protein interaction, and poly(ADP-ribose)-protein interactions.

Biological impact of Parp-1 *deficiency on gene expression relating to differentiation*

We observed genes involved in the pathway of extraembryonic tissue development, namely *H19*, *Sparc*, *Sox17*, *and Gata6*, are up-regulated in untreated *Parp-1*$^{-/-}$ ES cells (Table 3). In addition, during differentiation of ES cells after withdrawal of LIF, expression of *H19* as well as other trophoblast marker genes were further up-regulated in *Parp-1*$^{-/-}$ ES cells compared to *Parp-1*$^{+/+}$ ES cells (Fig. 4B). We previously reported that the increase of trophoblast marker genes, *Plf*, *Prlpa*, and *Tcfap2* was detected in untreated *Parp-1*$^{-/-}$ ES clone ($p < 0.05$) using GeneSpring 4.2 [15]. In the present paper, these genes were not picked up by GeneSpring 6.1 using two *Parp-1*$^{-/-}$ ES clones, probably because the criteria which we applied in this study were highly restricted and the expression level of the genes needed to be relatively high in at least one genotype. This is consistent with the fact that the gene expression changes associated with trophoblast induction were observed only in a subpopulation of ES cells by *in situ* hybridization [15]. In fact, *Plf* gene expression is not detectable in undifferentiated *Parp-1*$^{+/+}$ and *Parp-1*$^{-/-}$ ES cells by RT-PCR (Fig. 4B). In contrast, the differentially expressed genes picked up in the present study are expected to be the representative genes affected in a large cell population. *H19* is likely to be one of such genes in *Parp-1*$^{-/-}$ ES cells.

The biological function of *H19* RNA has not been fully understood yet. Several lines of evidence show that the *H19* gene is involved in extraembryonic tissue development as briefly mentioned earlier. The homozygous mutant animals with a targeted deletion of the maternal *H19* gene are viable and fertile and display an overgrowth phenotype of fetus and placentae compared with wild-type [41]. Mouse parthenogenetic embryos showing the monoallelic expression of the *H19* gene exhibit functional defects in placentae [18], suggesting that the *H19* gene may play an important role in the extraembryonic tissue development, especially in placentae.

Increased potential of *Parp-1*$^{-/-}$ ES cells to differentiation into trophoblasts seemed to reflect preferential differentiation of *Parp-1*$^{-/-}$ ES cells to trophoblasts triggered by LIF withdrawal, as shown in Fig. 4B. Early increase of *H19* expression suggests that the *H19* gene might act as an upstream regulator for the trophoblast differentiation pathway.

Conclusion

These results suggest that *Parp-1* is required to maintain transcriptional regulation of a wide variety of genes on a genome-wide scale. In *Parp-1*$^{-/-}$ ES cells and livers, we observed that the majority of the altered genes were down-regulated. These down- and up-regulated genes are involved in a variety of cellular processes, including transcription, metabolism, signaling, immune response, cell structure, and other cellular processes. In this study, we showed that the pathway of extraembryonic tissues including trophoblast lineage is potentially up-regulated at an untreated state and after differentiation stimuli in *Parp-1*$^{-/-}$ ES cells. The gene expression profiles in *Parp-1*-deficient cells may be useful to delineate the functional role of Parp-1 in epigenetic regulation of the genomes involved in various biological phenomena.

Methods

Cell lines and culture conditions

Parp-1$^{-/-}$ ES cell clones, 210-58 and 226-47, established independently from *Parp-1*$^{+/-}$ ES cells clones, 210 and 226, respectively, were used in this study [28]. They were all derived from male J1 ES cells. The ES cell lines were maintained in Dulbecco's modified Eagle's medium (Invitrogen) containing 20% fetal calf serum supplemented with amino acids and leukemia inhibitory factor (LIF), ESGRO (Chemicon) in the absence of a STO feeder, and total RNA was prepared as described below. Differentiation of ES cells by withdrawal of LIF was induced by inoculating 3×10^6 of ES cells in suspension in a culture dish (OPTILUX® Petri dish, Becton Dickinson) containing 10 ml of ES medium without LIF. Medium was changed at days 3 and 5. At days 3, 5, and 7, all the cells including floating embryoid bodies were collected. The livers were prepared from *Parp-1*$^{+/+}$ and *Parp-1*$^{-/-}$ female mice at 13 months of age [42], and about one-fifth of the amount of livers was used for total RNA extraction. Primary mouse embryonic fibroblasts (EFs) were derived from embryos at day 13.5 obtained by sister-brother mating of *Parp-1*$^{+/-}$ mice with a 129Sv/ICR mixed genetic background as previously described [43]. Briefly, each embryo was minced, trypsinized, and dispersed cells were incubated for 1 or 2 days until the EF cells became confluent. The EF cells were replated on four dishes and when they became confluent, these EF cells were defined to be at the 3 population doubling level (PDL). When the EF cells reached 6 PDL, they were harvested when they reached half confluency.

Total RNA isolation

Total RNA was extracted from ES cells, the livers, and EF cells using Isogen (Nippon Gene). Fifty micrograms of total RNA were treated with 5 units of DNase I (Invitrogen) for 15 min at room temperature, and purified again with Isogen.

Oligonucleotide microarray

Sample preparation and microarray processing were carried out according to the protocol supplied by Affymetrix. Briefly, 5 μg of total RNA sample treated with DNase I were reverse-transcribed by Superscript II reverse transcriptase (Invitrogen) using T7-$(dT)_{24}$ primer containing T7 RNA polymerase promoter sequence. After second-strand complementary DNA (cDNA) synthesis, the product was used in an *in vitro* transcription reaction to generate biotinylated complementary RNA (cRNA) using a BioArray™ HighYield™ RNA Transcript Labeling Kit (Enzo Diagnostics, Inc). Fifteen micrograms of fragmented cRNA were hybridized to a murine genome U74A version 2 micro-array (Affymerix) for 16–18 hours at 45°C with constant rotation at 60 rpm. This high-density oligonucleotide microarray contained 12,488 mouse genes/EST.

After hybridization, the microarray was washed and stained with streptavidin R-phycoerythrin conjugate using an Affymetrix Fluidics Station. The fluorescence intensity was measured twice for each microarray and the average fluorescence intensity was normalized by global scaling to 1,000. The data were saved in Microsoft Excel files, then imported into a GeneSpring® 6.1 software database (Silicon Genetics). The data sets for J1 and 210-58 (*Parp-1*$^{-/-}$) ES cells partially discussed in Hemberger *et al.* [15] were included in this study and further analyzed with GeneSpring® 6.1.

Data analysis

Data analysis was performed with the GeneSpring® 6.1 software. For statistical analyses, the fluorescence intensity (raw signal) was normalized to the median reading per chip, and then normalized to median reading per gene.

We used 6 replicates for each non-parametric tests with the global standard error model being inactive because more than five replicates were recommended for the tests. In the case of *Parp-1*$^{-/-}$ ES cells, 6 replicates consisting of triplicate microarray results from two *Parp-1*$^{-/-}$ ES cell lines were used. In the case of livers, 6 replicates consisting of triplicates obtained from two different animals, respectively, were used for each genotype. In the case of EF cells, 3 replicates obtained using three different embryos were used for each genotype and the global standard error model was active. We excluded those genes that showed a standard deviation greater than 2.0 in the normalized data of both genotypes, therefore, we started analysis with 9,907, 12,353, and 12,359 genes and ESTs for ES cells, livers, and EFs, respectively (Table 1). We constructed gene lists only with the genes that showed statistical differences ($p < 0.05$ or $p < 0.01$) and 2-fold or greater differences in normalized expression levels between *Parp-1* genotypes. To construct heatmaps, we used GeneSpring® GX ver. 7.3.1 (the latest version).

Northern blot analysis

Total RNA samples (10 μg) were used for northern blot analysis as described elsewhere [15]. We used the 90 bp (*Igfbp3*) or the 89 bp (*Galnt1*) cDNA fragment as a probe. The membrane was hybridized with the probe and was washed. The membrane was exposed to a Fuji Imaging Plate (Fuji film), and the radioactivities were analyzed using BAS-2500 Bio-imaging analyzer (Fuji film).

Reverse transcription polymerase chain reaction (RT-PCR)

We used Superscript™ III First-Strand Synthesis System for RT-PCR kit (Invitrogen). First-strand cDNA was synthesized from 2 μg each of DNase I-treated total RNA using an oligo$(dT)_{20}$ primer and Superscript™ III reverse transcriptase. After the first-strand cDNA synthesis, PCR amplification was performed using TAKARA Ex *Taq* (Takara Bio) with primers listed in Table S1 (see Additional file 1). The thermal cycle conditions were as follows: 94°C for 2 min, then 18 cycles (*Oct3/4*), 20 cycles (*Gapdh*), 22 cycles (Fig. 4B) or 24 cycles (Fig. 4A) (*H19* and *Igf2*). For *Cdx2*, 30 cycles at 94°C for 30 sec, 60°C for 30 sec, and 72°C for 30 sec were carried out. For *Plf*, 94°C for 2 min, then 40 cycles at 94°C for 30 sec, 68°C for 2 min 30 sec, and then 72°C for 3 min. Products were run on 1.5–3% agarose gel and stained with ethidium bromide. Confirmation of PCR products was carried out by direct sequencing.

Authors' contributions

HO, TN, TO, M. Maeda, HS, YM, HN, and M. Masutani designed the experiments. HO, TN, AG, M. Maeda, and M. Masutani performed the experiments. HO and M. Masutani prepared the manuscript. HS contributed to maintaining *Parp-1* knockout mice. M. Masutani, HN, and TS coordinated the project.

Additional material

Additional File 1

Table S1. Primers used in this study. Primers used in RT-PCR analysis (Fig. 4).

Click here for file

[http://www.biomedcentral.com/content/supplementary/1471-2164-8-41-S1.pdf]

Acknowledgements

This work was supported in part by Grant-in-Aids for the Second Term Comprehensive 10-Year Strategy for Cancer Control and a Grant-in-Aid for Cancer Research from the Ministry of Health, Labour and Welfare of Japan, and for the Third Term Comprehensive Control Research for Cancer from the Ministry of Health, Labour, and Welfare of Japan. HO and AG

were awardees of Research Resident Fellowships from the Foundation for Promotion of Cancer Research (Japan) for the Third Term Comprehensive 10-Year-Strategy for Cancer Control from the Ministry of Health, Labour and Welfare of Japan.

References

1. Sugimura T: **Poly(adenosine diphosphate ribose).** *Prog Nucleic Acid Res Mol Biol* 1973, **13**:127-151.
2. Realini CA, Althaus FR: **Histone shuttling by poly(ADP-ribosylation).** *J Biol Chem* 1992, **267(26)**:18858-18865.
3. Akiyama T, Takasawa S, Nata K, Kobayashi S, Abe M, Shervani NJ, Ikeda T, Nakagawa K, Unno M, Matsuno S, *et al.*: **Activation of *Reg* gene, a gene for insulin-producing beta-cell regeneration: poly(ADP-ribose) polymerase binds Reg promoter and regulates the transcription by autopoly(ADP-ribosyl)ation.** *Proc Natl Acad Sci USA* 2001, **98(1)**:48-53.
4. Sawatsubashi S, Maki A, Ito S, Shirode Y, Suzuki E, Zhao Y, Yamagata K, Kouzmenko A, Takeyama K, Kato S: **Ecdysone receptor-dependent gene regulation mediates histone poly(ADP-ribosyl)ation.** *Biochem Biophys Res Commun* 2004, **320(1)**:268-272.
5. Kannan P, Yu Y, Wankhade S, Tainsky MA: **PolyADP-ribose polymerase is a coactivator for AP-2-mediated transcriptional activation.** *Nucleic Acids Res* 1999, **27(3)**:866-874.
6. Cervellera MN, Sala A: **Poly(ADP-ribose) polymerase is a B-MYB coactivator.** *J Biol Chem* 2000, **275(14)**:10692-10696.
7. Miyamoto T, Kakizawa T, Hashizume K: **Inhibition of nuclear receptor signalling by poly(ADP-ribose) polymerase.** *Mol Cell Biol* 1999, **19(4)**:2644-2649.
8. Soldatenkov VA, Chasovskikh S, Potaman VN, Trofimova I, Smulson ME, Dritschilo A: **Transcriptional repression by binding of poly(ADP-ribose) polymerase to promoter sequences.** *J Biol Chem* 2002, **277(1)**:665-670.
9. Ha HC, Hester LD, Snyder SH: **Poly(ADP-ribose) polymerase-1 dependence of stress-induced transcription factors and associated gene expression in glia.** *Proc Natl Acad Sci USA* 2002, **99(5)**:3270-3275.
10. Simbulan-Rosenthal CM, Ly DH, Rosenthal DS, Konopka G, Luo R, Wang ZQ, Schultz PG, Smulson ME: **Misregulation of gene expression in primary fibroblasts lacking poly(ADP-ribose) polymerase.** *Proc Natl Acad Sci USA* 2000, **97(21)**:11274-11279.
11. Tulin A, Spradling A: **Chromatin loosening by poly(ADP)-ribose polymerase (PARP) at *Drosophila* puff loci.** *Science* 2003, **299(5606)**:560-562.
12. Kim MY, Mauro S, Gevry N, Lis JT, Kraus WL: **NAD$^+$-dependent modulation of chromatin structure and transcription by nucleosome binding properties of PARP-1.** *Cell* 2004, **119(6)**:803-814.
13. Zardo G, Caiafa P: **The unmethylated state of CpG islands in mouse fibroblasts depends on the poly(ADP-ribosyl)ation process.** *J Biol Chem* 1998, **273(26)**:16517-16520.
14. Nozaki T, Masutani M, Watanabe M, Ochiya T, Hasegawa F, Nakagama H, Suzuki H, Sugimura T: **Syncytiotrophoblastic giant cells in teratocarcinoma-like tumors derived from *Parp*-disrupted mouse embryonic stem cells.** *Proc Natl Acad Sci USA* 1999, **96**:13345-13350.
15. Hemberger M, Nozaki T, Winterhager E, Yamamoto H, Nakagama H, Kamada N, Suzuki H, Ohta T, Ohki M, Masutani M, *et al.*: ***Parp1*-deficiency induces differentiation of ES cells into trophoblast derivatives.** *Dev Biol* 2003, **257(2)**:371-381.
16. Poirier F, Chan CT, Timmons PM, Robertson EJ, Evans MJ, Rigby PW: **The murine *H19* gene is activated during embryonic stem cell differentiation *in vitro* and at the time of implantation in the developing embryo.** *Development* 1991, **113(4)**:1105-1114.
17. Rachmilewitz J, Gileadi O, Eldar-Geva T, Schneider T, de-Groot N, Hochberg A: **Transcription of the *H19* gene in differentiating cytotrophoblasts from human placenta.** *Mol Reprod Dev* 1992, **32(3)**:196-202.
18. Kono T, Sotomaru Y, Katsuzawa Y, Dandolo L: **Mouse parthenogenetic embryos with monoallelic *H19* expression can develop to day 17.5 of gestation.** *Dev Biol* 2002, **243(2)**:294-300.
19. Mason IJ, Taylor A, Williams JG, Sage H, Hogan BL: **Evidence from molecular cloning that SPARC, a major product of mouse embryo parietal endoderm, is related to an endothelial cell 'culture shock' glycoprotein of Mr 43,000.** *Embo J* 1986, **5(7)**:1465-1472.
20. Kanai-Azuma M, Kanai Y, Gad JM, Tajima Y, Taya C, Kurohmaru M, Sanai Y, Yonekawa H, Yazaki K, Tarn PP, *et al.*: **Depletion of definitive gut endoderm in *Sox17*-null mutant mice.** *Development* 2002, **129(10)**:2367-2379.
21. Koutsourakis M, Langeveld A, Patient R, Beddington R, Grosveld F: **The transcription factor GATA6 is essential for early extraembryonic development.** *Development* 1999, **126(9)**:723-32.
22. Gabory A, Ripoche MA, Yoshimizu T, Dandolo L: **The *H19* gene: regulation and function of a non-coding RNA.** *Cytogenet Genome Res* 2006, **113(1–4)**:188-193.
23. Robertson EJ: **Embryo-derived stem cell lines.** In *Teratocarcinomas and embryonic stem cells: a practical approach* Edited by: Robertson EJ. Oxford IR Press; 1987:71-112.
24. Leahy A, Xiong JW, Kuhnert F, Stuhlmann H: **Use of developmental marker genes to define temporal and spatial patterns of differentiation during embryoid body formation.** *J Exp Zool* 1999, **284(1)**:67-81.
25. Tanaka S, Kunath T, Hadjantonakis AK, Nagy A, Rossant J: **Promotion of trophoblast stem cell proliferation by FGF4.** *Science* 1998, **282(5396)**:2072-2075.
26. Lee SJ, Talamantes F, Wilder E, Linzer DI, Nathans D: **Trophoblastic giant cells of the mouse placenta as the site of proliferin synthesis.** *Endocrinology* 1988, **122(5)**:1761-1768.
27. Palmieri SL, Peter W, Hess H, Scholer HR: **Oct-4 transcription factor is differentially expressed in the mouse embryo during establishment of the first two extraembryonic cell lineages involved in implantation.** *Dev Biol* 1994, **166(1)**:259-267.
28. Masutani M, Nozaki T, Nishiyama E, Ochiya T, Nakagama H, Wakabayashi K, Suzuki H, Sugimura T: **Establishment of poly(ADP-ribose) polymerase-deficient mouse embryonic stem cell lines.** *Proc Japan Acad* 1998, **74B**:233-236.
29. Ogino H, Shibata A, Gunji A, Suzuki H, Nakagama H, Sugimura T, Masutani M: **Agent-dependent effects of *Parp-1* deficiency on DNA damage responses and genomic stability in mouse ES cells.** In *New Developments in Stem Cell Research* Edited by: Greer EV. New York: Nova Science Publishers; 2006:133-147.
30. Oei SL, Griesenbeck J, Schweiger M, Ziegler M: **Regulation of RNA polymerase II-dependent transcription by poly(ADP-ribosyl)ation of transcription factors.** *J Biol Chem* 1998, **273(48)**:31644-31647.
31. Nie J, Sakamoto S, Song D, Qu Z, Ota K, Taniguchi T: **Interaction of Oct-1 and automodification domain of poly(ADP-ribose) synthetase.** *FEBS Lett* 1998, **424(1–2)**:27-32.
32. Hassa PO, Buerki C, Lombard C, Imhof R, Hottiger MO: **Transcriptional coactivation of nuclear factor-kappaB-dependent gene expression by p300 is regulated by poly(ADP)-ribose polymerase-1.** *J Biol Chem* 2003, **278(46)**:45145-45153.
33. Dear TN, Hainzl T, Follo M, Nehls M, Wilmore H, Matena K, Boehm T: **Identification of interaction partners for the basic-helix-loop-helix protein E47.** *Oncogene* 1997, **14(8)**:891-898.
34. Butler AJ, Ordahl CP: **Poly(ADP-ribose) polymerase binds with transcription enhancer factor 1 to MCAT1 elements to regulate muscle-specific transcription.** *Mol Cell Biol* 1999, **19(1)**:296-306.
35. Pavri R, Lewis B, Kim TK, Dilworth FJ, Erdjument-Bromage H, Tempst P, de Murcia G, Evans R, Chambon P, Reinberg D: **PARP-1 determines specificity in a retinoid signaling pathway via direct modulation of mediator.** *Mol Cell* 2005, **18(1)**:83-96.
36. Idogawa M, Yamada T, Honda K, Sato S, Imai K, Hirohashi S: **Poly(ADP-ribose) polymerase-1 is a component of the oncogenic T-cell factor-4/beta-catenin complex.** *Gastroenterology* 2005, **128(7)**:1919-1936.
37. Galande S, Kohwi-Shigematsu T: **Poly(ADP-ribose) polymerase and Ku autoantigen form a complex and synergistically bind to matrix attachment sequences.** *J Biol Chem* 1999, **274(29)**:20521-20528.
38. Lonskaya I, Potaman VN, Shlyakhtenko LS, Oussatcheva EA, Lyubchenko YL, Soldatenkov VA: **Regulation of poly(ADP-ribose) polymerase-1 by DNA structure-specific binding.** *J Biol Chem* 2005, **280(17)**:17076-17083.
39. Herceg Z, Li H, Cuenin C, Shukla V, Radolf M, Steinlein P, Wang ZQ: **Genome-wide analysis of gene expression regulated by the HAT cofactor *Trrap* in conditional knockout cells.** *Nucleic Acids Res* 2003, **31(23)**:7011-7023.
40. Kraus WL, Lis JT: **PARP goes transcription.** *Cell* 2003, **113(6)**:677-683.
41. Ripoche MA, Kress C, Poirier F, Dandolo L: **Deletion of the *H19* transcription unit reveals the existence of a putative imprinting control element.** *Genes Dev* 1997, **11(12)**:1596-1604.
42. Nozaki T, Fujihara H, Watanabe M, Tsutsumi M, Nakamoto K, Kusuoka O, Kamada N, Suzuki H, Nakagama H, Sugimura T, *et al.*: ***Parp-1* deficiency implicated in colon and liver tumorigenesis induced by azoxymethane.** *Cancer Sci* 2003, **94(6)**:497-500.
43. Nozaki T, Fujihara H, Kamada N, Ueda O, Takato T, Nakagama H, Sugimura T, Suzuki H, Masutani M: **Hyperploidy of embryonic fibroblasts derived from *Parp-1* knockout mouse.** *Proc Jpn Acad* 2001, **77B**:121-124.

Ku70 and Poly(ADP-Ribose) Polymerase-1 Competitively Regulate β-Catenin and T-Cell Factor-4–Mediated Gene Transactivation: Possible Linkage of DNA Damage Recognition and Wnt Signaling

Masashi Idogawa,[1,3,4,5] Mitsuko Masutani,[2] Miki Shitashige,[1] Kazufumi Honda,[1] Takashi Tokino,[3] Yasuhisa Shinomura,[4] Kohzoh Imai,[4] Setsuo Hirohashi,[1] and Tesshi Yamada[1]

[1]Chemotherapy Division and [2]ADP-Ribosylation in Oncology Project, National Cancer Center Research Institute, Tokyo, Japan; [3]Department of Molecular Biology, Cancer Research Institute; [4]First Department of Internal Medicine; and [5]Department of Biomedical Engineering, Biomedical Research Center, Sapporo Medical University, Sapporo, Japan

Abstract

Formation of the T-cell factor-4 (TCF-4) and β-catenin nuclear complex is considered crucial to embryonic development and colorectal carcinogenesis. We previously reported that poly(ADP-ribose) polymerase-1 (PARP-1) interacts with the TCF-4 and β-catenin complex and enhances its transcriptional activity. However, its biological significance remains unexplained. Using immunoprecipitation and mass spectrometry, we found that two Ku proteins, Ku70 and Ku80, were also associated with the complex. Knockdown of Ku70 by RNA interference increased the amount of β-catenin associated with TCF-4 and enhanced the transcriptional activity. PARP-1 competed with Ku70 for binding to TCF-4. Treatment with bleomycin, a DNA-damaging alkylating agent, induced polyADP-ribosylation of PARP-1 protein and inhibited its interaction with TCF-4. Bleomycin conversely increased the amounts of Ku70 coimmunoprecipitated with TCF-4 and removed β-catenin from TCF-4. We propose a working model in which the transcriptional activity of TCF-4 is regulated by the relative amount of Ku70, PARP-1, and β-catenin proteins binding to TCF-4. Identification of the functional interaction of Ku70 as well as PARP-1 with the TCF-4 and β-catenin transcriptional complex may provide insights into a novel linkage between DNA damage recognition/repair and Wnt signaling. [Cancer Res 2007;67(3):911–8]

Introduction

The Wnt signaling pathway plays important roles in embryogenesis and carcinogenesis (1). Secreted Wnt molecules bind to cell membrane Frizzled receptors and evoke downstream intracellular signaling. The signal is then transmitted to a multiprotein complex consisting of the *APC* gene product, Axin/Axil, and glycogen synthase kinase 3β (GSK3β), a chaperone that supports the phosphorylation of β-catenin by GSK3β (2, 3). Phosphorylated β-catenin protein is subject to rapid degradation via the ubiquitin-proteasome pathway (4). The Wnt signaling inhibits GSK3β and increases the cytoplasmic β-catenin content. Mutation of either the *APC* or β-catenin (*CTNNB1*) gene is frequently seen in colorectal carcinoma and mimics the constitutively active Wnt signaling (5, 6). The excess β-catenin protein acts as a transcriptional coactivator by forming complexes with T-cell factor (TCF)/lymphoid enhancer factor (LEF) family DNA-binding proteins (7). TCF-4 is a member of the TCF/LEF family commonly expressed in colorectal epithelium and cancer cells (8). TCF-4 has been implicated in the maintenance of undifferentiated intestinal crypt epithelial cells because no proliferative compartments have been detected in the intestinal crypts of mice lacking TCF-4 (9). Constitutive transactivation of the target genes of TCF-4 by accumulation of β-catenin protein imposes a crypt progenitor phenotype on intestinal epithelial cells and is considered crucial to the initiation of colorectal carcinogenesis (10).

In our previous study, we found that poly(ADP-ribose) polymerase-1 (PARP-1) interacted with the TCF-4 and β-catenin nuclear complex (11). PARP-1 was originally identified as a nuclear DNA-binding protein that catalyzes the transfer of ADP-ribose from NAD^+ to acceptor proteins (12). PARP-1 is activated by DNA damage and plays an important role in the process of DNA repair and genomic stability (13).

Besides DNA damage recognition and apoptosis, the role of PARP-1 as a regulator of various transcription factors has recently attracted a great deal of attention (14). We have found that PARP-1 is a component and enhancer of the TCF-4 and β-catenin transcriptional complex (11). PARP-1 polyADP-ribosylates its own automodification domain in response to DNA damage (12). PolyADP-ribosylation of PARP-1 inhibits the interaction with TCF-4 and its transcriptional activity (11). However, the biological significance of the interaction between TCF-4 and PARP-1 and its inhibition by polyADP-ribosylation of PARP-1 remains unexplained.

In this study, we further explored the protein components of the TCF-4 and β-catenin nuclear complex and identified that Ku70 and Ku80 proteins interact with TCF-4. The Ku autoantigen was originally identified as a nuclear protein recognized by autoantibodies in sera of patients with polymyositis-scleroderma overlap syndrome (15). The Ku autoantigen consists of two subunit proteins of ~70 kDa and 80 to 86 kDa (named Ku70 and Ku80). Ku recognizes DNA double strand breaks and then recruits the DNA-dependent protein kinase catalytic subunit (DNA-PKcs; ref. 16). The Ku70/Ku80/DNA-PKcs complex mediates nonhomologous end joining and repairs double strand breaks (17). Ku proteins are also involved in other cellular processes such as immunoglobulin gene rearrangement, telomere maintenance, apoptosis, and transcriptional regulation (18). Here, we report that Ku70 is a novel inhibitor of the β-catenin/TCF-4 transcriptional complex.

Note: Supplementary data for this article are available at Cancer Research Online (http://cancerres.aacrjournals.org/).

Requests for reprints: Tesshi Yamada, Chemotherapy Division, National Cancer Center Research Institute, 5-1-1 Tsukiji, Chuo-ku, Tokyo 104-0045, Japan. Phone: 81-3-3542-2511, ext. 4270; Fax: 81-3-3547-6045; E-mail: tyamada@gan2.res.ncc.go.jp.

doi:10.1158/0008-5472.CAN-06-2360

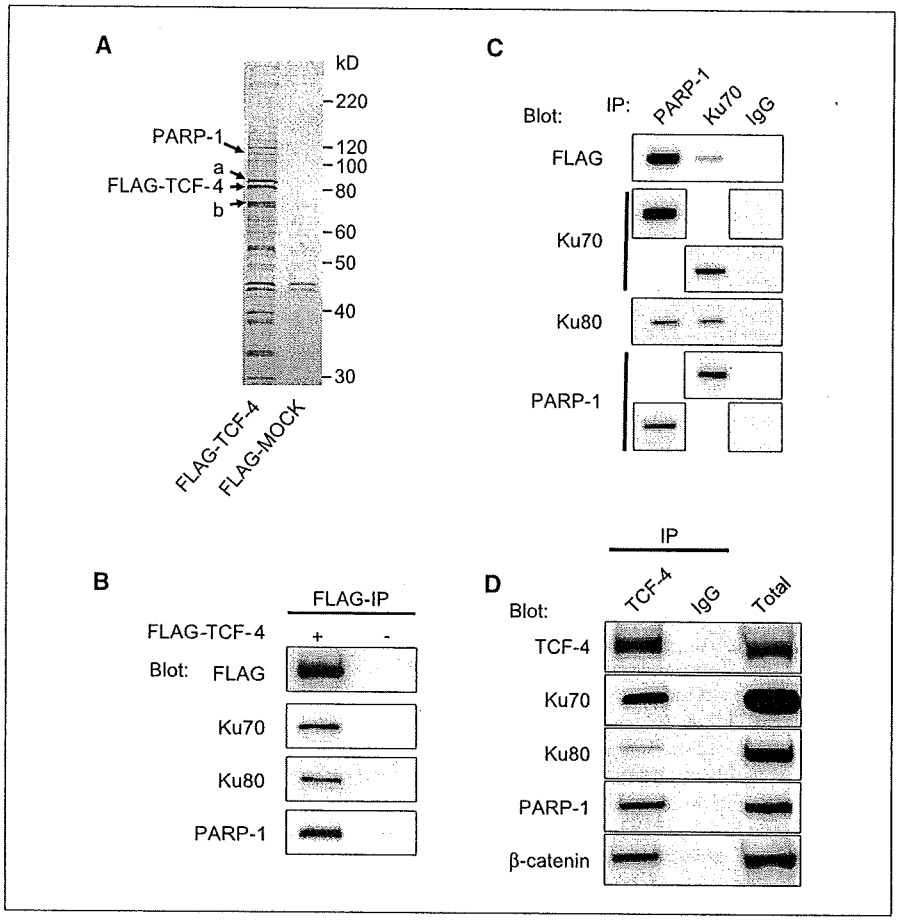

Figure 1. Identification of interaction between Ku and TCF-4. *A*, HEK293 cells were transfected with FLAG–TCF-4 or control FLAG-MOCK. Nuclear extracts were immunoprecipitated with anti-FLAG affinity gel (modified from ref. 11 with permission). *B*, Western blot analysis of the immunoprecipitates (*IP*) of HEK293 cells transfected with FLAG–TCF-4 (+) or control FLAG-MOCK (–). The immunoprecipitates with anti-FLAG affinity beads were blotted with anti-FLAG, anti-Ku70, anti-Ku80, and anti–PARP-1 antibodies. *C*, lysate of HEK293 cells transfected with FLAG–TCF-4 was immunoprecipitated with anti–PARP-1 and anti-Ku70 antibody or normal mouse IgG and blotted with anti-FLAG, anti-Ku70, anti-Ku80, and anti–PARP-1 antibodies. *D*, nuclear extract of HCT116 cells (*Total*) was immunoprecipitated with anti–TCF-4 antibody or normal mouse IgG and blotted with anti–TCF-4, anti-Ku70, anti-Ku80, anti–PARP-1, and anti–β-catenin antibodies.

Materials and Methods

Cell culture. The human embryonal kidney cell line HEK293 was obtained from the Riken Cell Bank (Tsukuba, Japan). Hepatoblastoma cell line HepG2 and colorectal cancer cell lines HCT116, DLD-1, and SW480 were purchased from the American Type Culture Collection (Manassas, VA). The Li7 cell line was established from a patient with hepatocellular carcinoma as reported previously (19). PARP-null mouse embryonic fibroblast (MEF) was established from a PARP-1 knockout (*Parp1*$^{-/-}$) mouse (20).

Cells were treated with 5 mmol/L hydroxyurea (Sigma, St. Louis, MO) for 18 h at 37°C. The medium was then removed, and incubation was continued with serum-free medium without or with bleomycin (50 μg/mL; Sigma).

Plasmid constructs. Human TCF-4 cDNA and its truncated forms were subcloned into pFLAG-CMV4 (Sigma). Human Ku70 cDNA and its truncated forms were subcloned into pcDNA3.1/myc-His (Invitrogen, Carlsbad, CA). Human PARP-1 cDNA (kindly provided by Dr. M. Miwa, Nagahama Institute of Bio-Science and Technology, Nagahama, Japan) was subcloned into pcDNA3.1/myc-His. Human β-cateninΔN134 cDNA was subcloned into pCR3.1 (Invitrogen), which lacks a 134-amino-acid sequence at its NH_2 terminus. The composition of all of the constructs in this study was confirmed by restriction endonuclease digestion and sequencing.

Immunoprecipitation. Cells were extracted with lysis buffer [50 mmol/L Tris-HCl (pH 7.4), 150 mmol/L NaCl, 1 mmol/L EDTA, 1% Triton X-100] containing a protease inhibitor cocktail (Sigma). Nuclear extracts were prepared with the CelLytic nuclear extraction kit (Sigma). Immunoprecipitation was done with 50 μL of anti-FLAG M2 affinity gel (Sigma) or anti–PARP-1 monoclonal antibody (BD PharMingen, San Diego, CA), anti-Ku70 (Ab-5) monoclonal antibody (Lab Vision, Fremont, CA), and anti–TCF-4 monoclonal antibody (Upstate, Charlottesville, VA) along with 10 μL of Dynabeads Protein G (Dynal, Oslo, Norway). After being washed with washing buffer [50 mmol/L Tris-HCl (pH 7.4), 150 mmol/L NaCl], immobilized immunocomplexes were eluted from anti-FLAG M2 affinity gel by incubation at 4°C with 150 ng/μL 3×FLAG Peptide (Sigma) or from Dynabeads by boiling in SDS loading buffer. Proteins were fractionated by SDS-PAGE and detected using a negative gel stain MS kit (Wako, Osaka, Japan) or by Western blotting.

Protein identification by mass spectrometry. SDS-PAGE gels were cut into ~1-mm^3 sections, reduced with NH_4HCO_3, and alkylated with iodoacetamide. The gel sections were then washed with acetonitrile, hydrolyzed with modified trypsin (Promega, Madison, WI), and incubated at 37°C overnight. Peptides eluted from the gel sections were spotted onto a steel target plate along with 2,5-dihydroxybenzoic acid (gentisic acid; Sigma) as a matrix. Mass spectra were obtained in the refractor mode by using a Q-star Pulsar-*i* mass spectrometer (Applied Biosystems, Foster City, CA) and analyzed using Mascot software (Matrix Sciences, London, United Kingdom; ref. 21).

Western blot analysis. Anti–FLAG M2 monoclonal antibody was purchased from Sigma; anti-Ku70 (Ab-4) and anti-Ku80 (Ab-2) monoclonal antibodies were from Lab Vision; anti–β-catenin monoclonal antibody was from BD Transduction (Lexington, KY); anti-TCF3/4 monoclonal antibody was from Upstate; and anti-PARP polyclonal antibody was from Trevigen (Gaithersburg, MD). Total cell lysates were extracted at 4°C with radioimmunoprecipitation assay buffer [150 mmol/L NaCl, 1% NP40, 0.5% sodium deoxycholate, 0.1% SDS, 50 mmol/L Tris-HCl (pH 8.0)]. Samples were

fractionated by SDS-PAGE and transferred onto Immobilon-P membranes (Millipore, Billerica, MA), and the blots were detected using an enhanced chemiluminescence method (Amersham, Piscataway, NJ).

Reverse transcription-PCR. Total RNA was prepared with an RNeasy mini kit (Qiagen, Valencia, CA), and 1-μg samples of total RNA were reverse transcribed. cDNA samples from tissues of human sporadic colorectal cancer and the corresponding normal tissues were obtained from Clontech (Palo Alto, CA). The PCR products were analyzed by agarose gel electrophoresis. The sequences of all the PCR primers in this study are available upon request.

Luciferase reporter assay. A pair of luciferase reporter constructs, TOP-FLASH and FOP-FLASH (Upstate), were used to evaluate TCF/LEF transcriptional activity. Cells were transiently transfected in triplicate with one of the luciferase reporters and phRG-TK (Promega) using Lipofectamine 2000 reagent (Invitrogen). Luciferase activity was measured with the Dual-luciferase reporter assay system (Promega) and *Renilla* luciferase activity as an internal control.

RNA interference. Two short hairpin RNA (shRNA) sequences targeting Ku70 mRNA were designed by B-Bridge (Sunnyvale, CA). Synthesized double-stranded oligonucleotides were cloned into the pSUPER RNA interference vector (OligoEngine, Seattle, WA) carrying the H1 promoter and neomycin resistance gene.

Immunofluorescence microscopy. Cells were grown on poly-L-lysine–coated coverslips (Asahi Technoglass, Funabashi, Japan). After being fixed with 3.7% paraformaldehyde, the cells were incubated with anti-PARP rabbit polyclonal antibody and anti-PARP-1 mouse monoclonal antibody (BD Transduction) overnight at 4°C. Following incubation with Alexa Fluor 488–labeled goat anti-mouse IgG and Alexa Fluor 594–labeled goat anti-rabbit IgG (Molecular Probes, Eugene, OR), the coverslips were inspected with a laser scanning confocal microscope (Bio-Rad, Hercules, CA).

Immunohistochemistry. Ten familial adenomatous polyposis (FAP) patients were selected from the surgical pathology panel of the National Cancer Center Central Hospital. Formalin-fixed and paraffin-embedded intestinal tissues containing adenomas were stained by the avidin-biotin complex method as previously described (22).

Results

Identification of a novel interaction between the TCF-4 and Ku proteins. HEK293 cells were transiently transfected with FLAG-tagged TCF-4 (FLAG–TCF-4) or a control plasmid (FLAG-MOCK). Immunoprecipitation with anti-FLAG antibody and SDS-PAGE revealed that several proteins were selectively coimmunoprecipitated with FLAG–TCF-4, but not with the control (Fig. 1*A*). We had

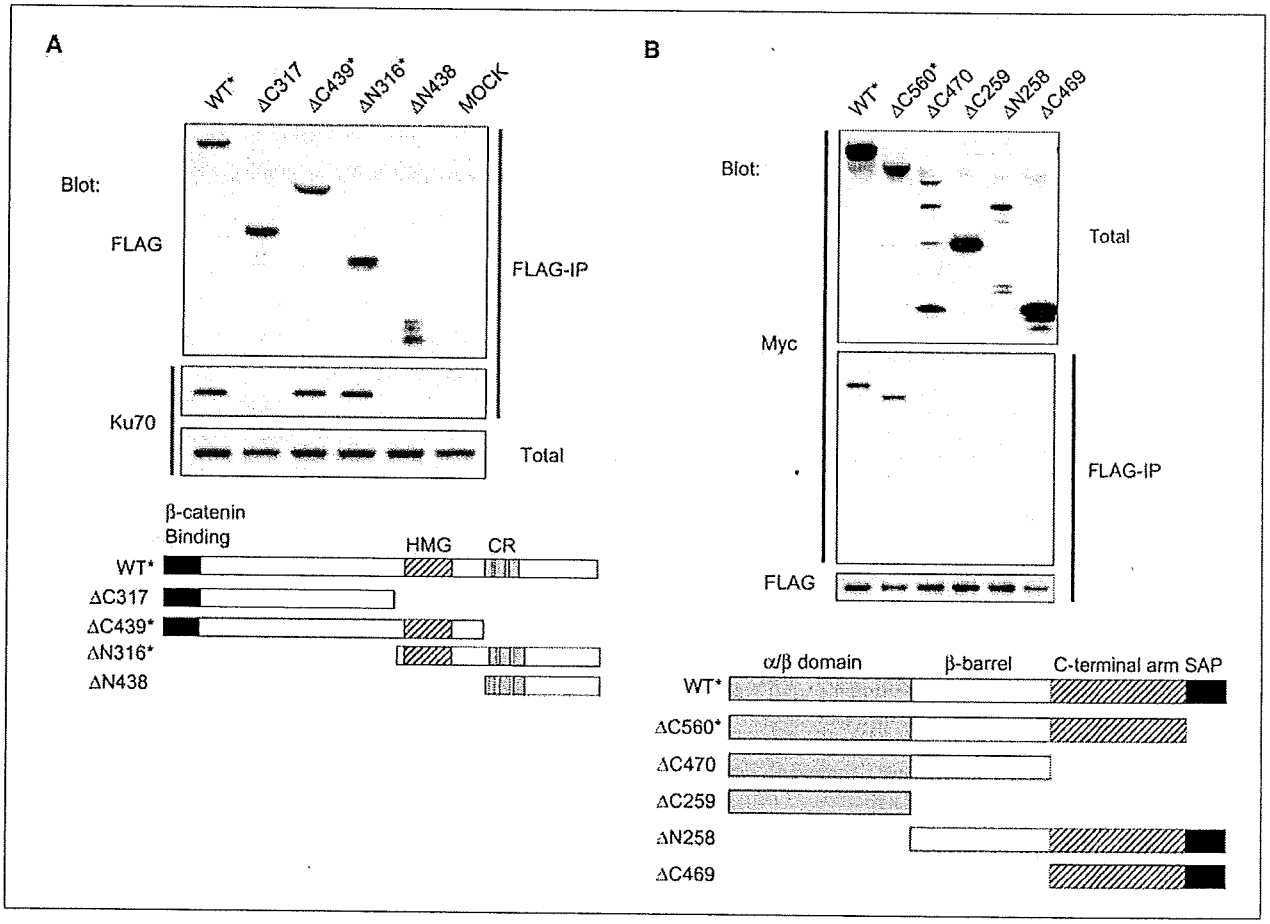

Figure 2. Binding domains necessary for interaction between Ku70 and TCF-4. *A*, full-length or truncated forms of FLAG–TCF-4 were transfected into HEK293 and immunoprecipitated with anti-FLAG affinity beads. The complexes were analyzed by blotting with anti-FLAG and anti-Ku70 antibodies. The full-length and truncated forms of TCF-4 are represented schematically at the bottom. *, TCF-4 constructs that bound to the Ku70 protein. *B*, Myc-tagged full-length or truncated forms of pcDNA3.1-Ku70 and full-length FLAG–TCF-4 were cotransfected into HEK293 and immunoprecipitated with anti-FLAG affinity beads. The complexes were analyzed by blotting with anti-Myc and anti-FLAG antibodies. The full-length and truncated forms of Ku70 are represented schematically at the bottom. *, Ku70 constructs that bound to the TCF-4 protein.

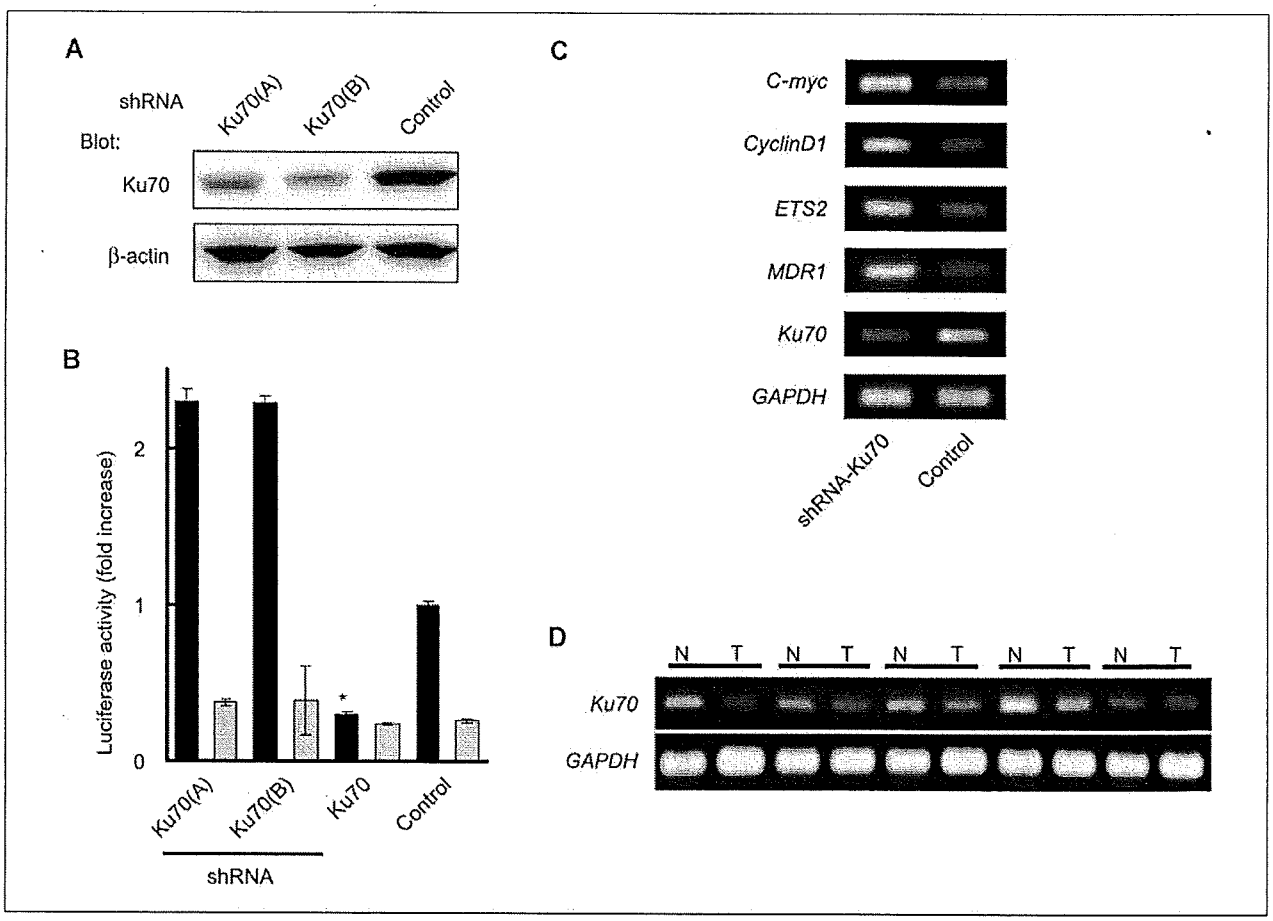

Figure 3. Ku70 suppresses gene transcriptional activity of TCF-4. *A*, Western blot analysis showing the protein level of Ku70 (*top*) and β-actin (loading control, *bottom*) of HCT116 cells transfected with pSUPER-Ku70 [*Ku70(A), Ku70(B)*] or pSUPER-control (*Control*). *B*, HCT116 cells were cotransfected with pSUPER-Ku70(A), pSUPER-Ku70(B), pcDNA3.1-Ku70 (*Ku70*), or control plasmid as well as canonical (TOP-FLASH) or mutant (FOP-FLASH) TCF/LEF luciferase reporter. Forty-eight hours after transfection, the luciferase activity of TOP-FLASH (*black columns*) and FOP-FLASH (*gray columns*) was measured. Activity was adjusted to the TOP-FLASH activity of the control transfectant and expressed as a fold increase. *C*, HCT116 cells were transiently transfected with a mixture of pSUPER-Ku70(A) and pSUPER-Ku70(B) (*shRNA-Ku70*) or empty pSUPER (*Control*). Forty-eight hours after transfection, the expression levels of *c-myc, cyclin D1, ETS2, MDR1, Ku70*, and *GAPDH* mRNA were analyzed by reverse transcription-PCR. *D*, expression of Ku70 and GAPDH mRNA in paired samples of normal intestine (*N*) and cancer (*T*) tissues from five patients with sporadic colorectal cancer.

previously identified one of these proteins as PARP-1 (Fig. 1*A*). Proteins of ~70 kDa (Fig. 1*A, b*) and 86 kDa (Fig. 1*A, a*) were also constantly coimmunoprecipitated with FLAG-tagged TCF-4 and were subjected to protein identification by mass spectrometry. Peptide mass fingerprinting and tandem mass spectrometry (data not shown) revealed that these proteins were Ku70 (70-kDa thyroid autoantigen/thyroid-lupus autoantigen/G22P1) and Ku80 (X-ray repair, complementing defective, in Chinese hamster, 5/XRCC5).

The protein identification was confirmed by Western blotting with anti-Ku70 and anti-Ku80 antibodies. Ku70, Ku80, and PARP-1 proteins were detected in the immunoprecipitate with anti-FLAG antibody (Fig. 1*B*). Ku70, Ku80, and FLAG-tagged TCF-4 proteins were detected in the immunoprecipitate with anti–PARP-1 antibody (Fig. 1*C, IP: PARP-1*). FLAG-tagged TCF-4 (FLAG), Ku80, and PARP-1 were also detected in the immunoprecipitate with anti-Ku70 antibody (Fig. 1*C, IP: Ku70*) but not with control mouse IgG (Fig. 1*C, IP: IgG*).

Ku70, Ku80, PARP-1, and β-catenin proteins were coimmunoprecipitated with endogenous TCF-4 from a lysate of colorectal cancer HCT116 cells (Fig. 1*D*). Ku70 and Ku80 were also coimmunoprecipitated with PARP-1 (Supplementary Fig. S1), suggesting that Ku70, Ku80, and PARP-1 are native components of the TCF-4 and β-catenin complex.

Binding domains necessary for the interaction between Ku70 and TCF-4. To identify the region of TCF-4 that is essential for its interaction with Ku70, we expressed serially truncated forms of FLAG–TCF-4 and evaluated their binding activity to Ku70 (Fig. 2*A*). Only constructs carrying the high-mobility group (HMG) box [wild-type (WT), ΔC439, and ΔN316] were found to bind to Ku70 (Fig. 2*A*).

The Ku70 protein consists of four domains: the α/β domain, β-barrel, COOH-terminal arm, and scaffold attachment factor (SAP) DNA-binding domain (23). We evaluated the ability of Ku70 serially truncated at the border of each domain to bind to FLAG–TCF-4 (Fig. 2*B*). Only the full-length Ku70 protein (WT) and the Ku70 protein lacking the SAP domain (ΔC560) interacted with TCF-4 (Fig. 2*B*). These results suggest that the three-dimensional structure of Ku70 protein rather than the specific amino acid

sequence is necessary for the interaction with TCF-4. It has been consistently reported that Ku70 needs to retain its three-dimensional structure to interact with Ku80, DNA, and other proteins (23).

Ku70 suppresses TCF-4–mediated gene transcriptional activity. To investigate the functional involvement of Ku proteins in the TCF-4 and β-catenin transcriptional complex, we knocked down the expression of Ku70 using shRNA. The decreased expression of Ku70 was confirmed by Western blotting (Fig. 3*A*). The knockdown of Ku70 expression increased the luciferase activity of TOP-FLASH, the canonical reporter of TCF/LEF transcriptional activity, ~2-fold over mock transfection (Fig. 3*B, black columns*) but did not affect significantly that of the mutant reporter FOP-FLASH (Fig. 3*B, gray columns*). Conversely, overexpression of Ku70 by cDNA transfection suppressed the TOP-FLASH activity ~4-fold (Fig. 3*B*, *, *Ku70*). Unlike Ku70, however, knockdown of Ku80 expression did not significantly affect the TOP-FLASH or FOP-FLASH activity (data not shown). Similar enhancement of TCF/LEF transcriptional activity by knockdown of Ku70 was observed in HepG2 and Li7 cells (Supplementary Fig. S2).

Consistent with the reporter assay, knockdown of Ku70 expression by transfection of shRNA into HCT116 cells increased the expression of known downstream target genes of TCF-4, including *c-myc* (*MYC*), *cyclin D1* (*CCND1*), *ETS2*, and *MDR1* (*ABCB1*; Fig. 3*C*). The expression of Ku70 mRNA in cancer tissues (*T*) was clearly decreased in four of five cases of sporadic colorectal cancer in comparison with the corresponding normal tissues (*N*, Fig. 3*D*).

Competitive regulation of the TCF-4 and β-catenin complex by Ku70 and PARP-1. Because PARP-1 has been reported to

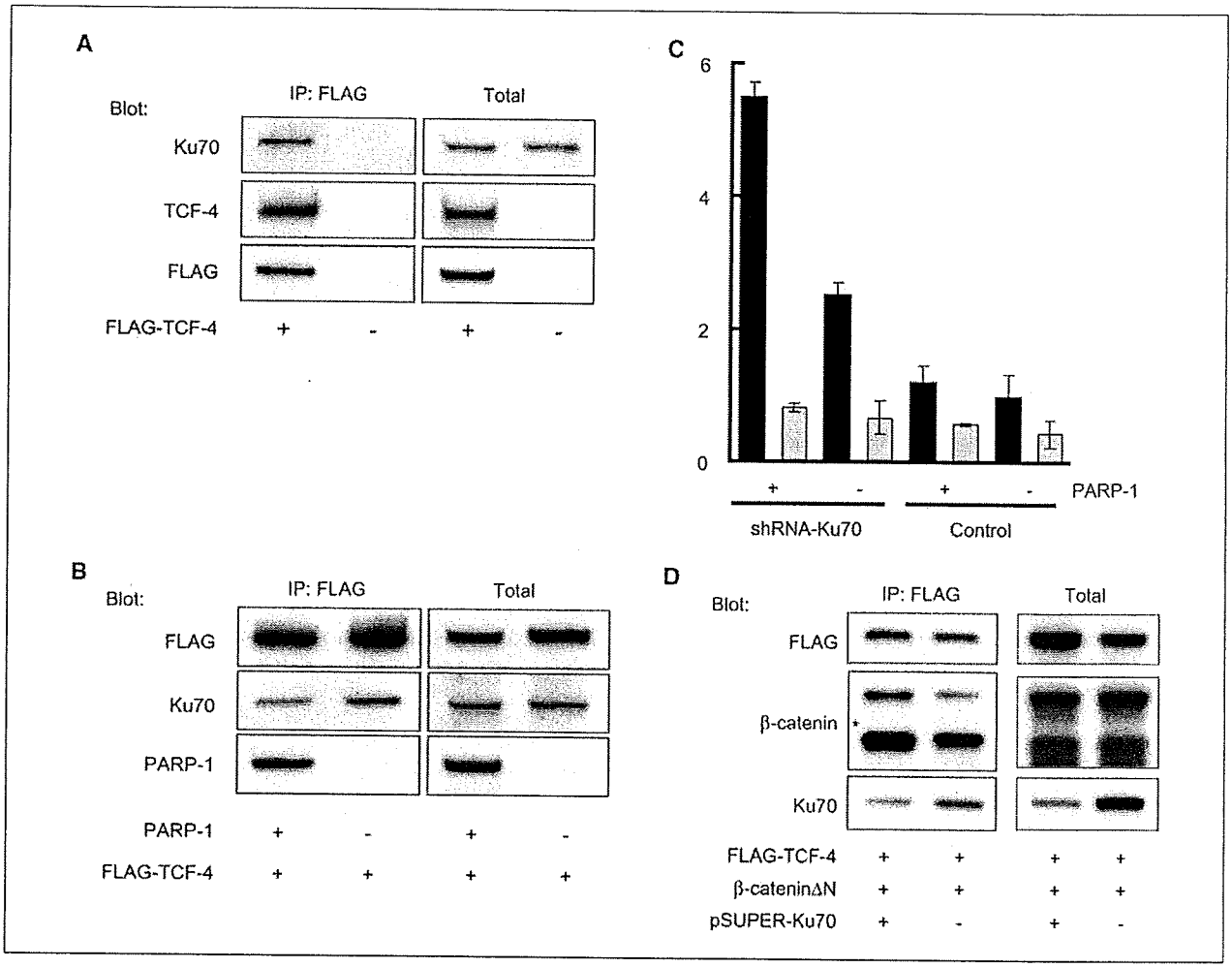

Figure 4. Competitive regulation of the TCF-4 and β-catenin complex by Ku70 and PARP-1. *A*, PARP-1–null MEF were transfected with FLAG–TCF-4 or FLAG-MOCK, and whole lysates (*Total*) and immunoprecipitates with anti-FLAG affinity beads (*IP: FLAG*) were blotted with anti-Ku70, anti-TCF-4, and anti-FLAG antibodies. *B*, PARP-1–null MEF were transfected with FLAG–TCF-4 and pcDNA3.1–PARP-1 or control pcDNA3.1. Whole lysates and immunoprecipitates with anti-FLAG affinity beads were blotted with anti-FLAG, anti-Ku70, and anti–PARP-1 antibodies. *C*, HCT116 cells were cotransfected with a mixture of pSUPER-Ku70(A) and pSUPER-Ku70(B) or empty pSUPER (*Control*) as well as pcDNA3.1-PARP-1 [*PARP-1*(+)] or empty pcDNA3.1/myc-His [*PARP-1*(−)] along with TOP-FLASH or FOP-FLASH luciferase reporter. Forty-eight hours after transfection, the luciferase activity of TOP-FLASH (*black columns*) and FOP-FLASH (*gray columns*) was measured. Activity was adjusted to the TOP-FLASH activity of the control transfectant [*Control, PARP-1*(−)] and expressed as a fold increase. *D*, HEK293 cells were transfected with FLAG–TCF-4, β-cateninΔN134, and a mixture of pSUPER-Ku70(A) and pSUPER-Ku70(B) (+) or empty pSUPER (−). Total cell lysates were immunoprecipitated with anti-FLAG affinity beads and blotted with anti-FLAG, anti–β-catenin, and anti-Ku70 antibodies.